THE JOURNAL OF NAVIGATION (2006), **59**, 395–401. © The Royal Institute of Navigation
doi:10.1017/S0373463306003821 Printed in the United Kingdom

Electron Density Profiles Derived From Ground-Based GPS Observations

Shuanggen Jin[1], J.U. Park[1], J.L. Wang[2], B.K. Choi[1] and P.H. Park[1]

(*Korea Astronomy and Space Science Institute, South Korea*[1] *, School of Surveying and Spatial Information System, University of New South Wales, Australia*[2])
(Email: sgjin@kasi.re.kr; sg.jin@yahoo.com)

Nowadays GPS is widely used to monitor the ionosphere. However, the current results from ground-based GPS observations only provide some information on the horizontal structure of the ionosphere, and are extremely restricted in mapping its vertical structure. In this paper, tomography reconstruction technique was used to image 3D ionospheric structure with ground-based GPS. The first result of the 3D images of the ionospheric electron density distribution in South Korea has been generated from the permanent Korean GPS Network (KGN) data. Compared with the profiles obtained by independent ionosondes at or near the GPS receiver stations, the electron density profiles obtained by the GPS tomographic construction method are in better agreement, showing the validity of the GPS ionospheric tomographic reconstruction. It has also indicated that GPS-based 3D ionospheric mapping has the potential to complement other expensive observing techniques in ionospheric mapping, such as ionosondes and radar.

KEY WORDS

1. Electron density. 2. Tomography reconstruction. 3. GPS.

1. INTRODUCTION. The ionosphere is about 60–1000 km above the earth's surface; it is a plasma of gas in the upper atmosphere ionized by solar radiation and high energy particles from the Sun. The ionized electron concentrations change with height above the earth's surface, location, time of the day, season, and the amount of solar activity, and the electron density is an important physical parameter in the ionosphere. Therefore, imaging the electron density is very crucial to determine the state of the ionospheric activities. In addition, the electron density profile in the Earth's ionosphere and plasmasphere is important for the estimation and correction of propagation delays in GPS, and for predicting space weather and ionospheric disturbances due to geomagnetic storms and solar flares.

In the past decades, different observing instruments, such as ionosonde, scatter radars (Tsunoda, 1988), topside sounders onboard satellites (Reinishch et al., 2001), in situ rocket and satellite observations (Klobuchar, 1991), and LEO GPS occultation

measurements (Jakowski et al., 2002), have been developed and used to gather information on the ionosphere and plasmasphere. But the instruments are restricted to either the bottomside ionosphere (ionosondes) or the lower part of the topside ionosphere (usually lower than 800 km), such as ground-based radar measurements. Satellites in high altitude orbits (e.g. GPS at ~20,200 km) are capable of providing details on the structure of the entire topside ionosphere, and the plasmasphere. Additionally, GPS is a low-cost, all-weather, near real time, and high-temporal resolution (30 s) technique (Klobuchar, 1991). Therefore, GPS has become the most widely used method for investigations of ionospheric irregularities. However, in the past, most scientists have used ground-based GPS data to monitor ionospheric irregularities based on a single layer model (SLM) of the ionosphere at the altitude of electron density peak, which is generally 350 km above the Earth (Schaer, 1999, Otsuka et al., 2002; Afraimovich et al., 2000 and 2004). In fact, the single layer model ignores the vertical variation information of the ionosphere. Therefore, to better monitor the ionospheric activities in full dimensions, it is a new challenge to map 3D ionosphere with GPS.

Austen et al (1988) first proposed the possibility of studying the ionosphere using satellite radio tomography and tomographic reconstruction techniques have been applied recently to ionospheric imaging. Computer aided tomography is a well known technique in medicine, where two dimensional cross section images of the body are derived from measurements of the attenuation of X-rays passing through a human body from many different angles. In X-ray tomography the attenuation is proportional to the line integral of the X-ray absorption along the ray path through the body. Tomographic imaging of ionospheric electron density involves measurements of the total electron content (TEC) along trans-ionospheric ray paths between global positioning satellites (GPS) and ground-based receivers. In computerized ionospheric tomography (CIT) the line integrals comprise the slant TEC (STEC) of GPS ray path. Therefore, using ground-based GPS STEC measurements and computerized ionospheric tomography it is possible to get 3D ionospheric structures. In this paper, we aim to map 3D ionospheric electron density distribution using ground-based GPS measurements with an ionospheric tomography method. The first reconstruction results of the electron density distribution in South Korea are presented using the permanent Korean GPS network (KGN). Finally the reconstructed electron density is verified by comparison with the independent observed results from ionosonde.

2. IONOSPHERIC RECONSTRUCTION METHOD.

GPS covers the globe with 24 hours operation and high temporal resolution (30 s intervals). Therefore, GPS can offer high sampling rate information on the ionosphere at many ray-path orientations. To achieve an accurate tomography of the ionospheric electron distribution, it is first necessary to get precise line-of-sight TEC from ground-based dual-frequency GPS measurements. The determination of TEC from GPS observations involves the measurement of the differential group delays (dispersive and non-dispersive) between the two frequencies. The instrumental (receiver and transmitter) dispersive delay, known as instrumental biases, can be removed by appropriate calibration of the transmitters and receivers. The difference equations of phase and code observations of double frequency GPS can be

expressed as follows:

$$\begin{aligned} \phi_{kj}^{i} &= R_{j}^{i} - \alpha_k I_{j}^{i} - \lambda_k (b_{kj}^{i} + N_{kj}^{i}) \\ P_{kj}^{i} &= R_{j}^{i} + \alpha_k I_{j}^{i} + dq_{kj} + dq_{k}^{i} \end{aligned} \tag{1}$$

Where a_k at $40{\cdot}3/f_k^2 (k=1, 2)$, λ_k is the wave length of frequency f_k, i and j represent the number of satellite and receiver respectively, ϕ_{kj}^{i} and P_{kj}^{i} stand for the phase and code observations, R_j^i is the sum of true distance, troposphere delay and clock bias correction, I_j^i is the ionospheric delay, b_{kj}^i is the phase delay of satellite and receiver instrument bias, dq_{kj} and dq_k^i are the group delay of satellite and receiver instrument bias respectively, and N_{kj}^i is the integer ambiguity. One can easily obtain the following equation from Equation (1)

$$L_4 = \phi_{1j}^{i} - \phi_{2j}^{i} = -40{\cdot}3\left(\frac{1}{f_1^2} - \frac{1}{f_2^2}\right) STEC + B_4 \tag{2}$$

$$P_4 = P_{1j}^{i} - P_{2j}^{i} = 40{\cdot}3\left(\frac{1}{f_1^2} - \frac{1}{f_2^2}\right) STEC + b_4 \tag{3}$$

Where *STEC* is the slant total electron content of GPS signal ray path, $B_4 = -\lambda_1(b_{1j}^{i} + N_{1j}^{i}) + \lambda_2(b_{2j}^{i} + N_{2j}^{i})$, and b_4 is $(dq_{1j} - dq_{2j}) + (dq_1^i - dq_2^i)$. The Differential Code Biases (b_4) can be estimated as constant values for each day from GPS observations, and B_4 can be obtained through the formula, $\sum_{i=1}^{N}(p_4 + L_4 - b_4)/N$, where N is the epoch of GPS observation. Thus, the *STEC* can be obtained (Jin et al., 2004). The *STEC* is defined as the line integral of the electron density as expressed by

$$STEC = \int_{R_{receiver}}^{R_{satellite}} N_e(\lambda, \varphi, h) ds \tag{4}$$

where $N_e(\lambda, \varphi, h)$ is the ionospheric electron density, λ, φ and h are the longitude, latitude and height, respectively. To get N_e, the ionosphere is divided into grid pixels with a small cell, assuming that the electron density is constant in each pixel, and thus the STEC along the ray path can be represented as a finite sum of shorter integrals along segments of the ray path length. Each set of STEC measurements along the ray paths from all observable satellites can form the following matrix:

$$Y = Ax + \varepsilon \tag{5}$$

where Y is a column of m measurements for STEC, x is a column of n electron density unknowns for cells in the targeted ionosphere region, and A is an $m \times n$ normal matrix with a_{ji}. The tomography algorithms are described in different ways, such as singular value decomposition (Wall et al., 2001), correlation function (Ruffini et al., 1998), algebraic reconstruction technique (ART) (Gordon et al., 1970) etc. One of the most commonly used approaches is the algebraic reconstruction technique (ART) which was first introduced in Computerized Ionospheric Tomography (CIT) by Austen et al. (1988). This is an iterative procedure for solving a linear equation. A modified version of ART is the so-called multiplicative ART (MART) and the correction in each iteration is obtained by making a multiplicative modification to x rather than an additive correction (Raymund et al., 1990; Tsai et al., 2002). MART has an advantage over ART in determining the electron

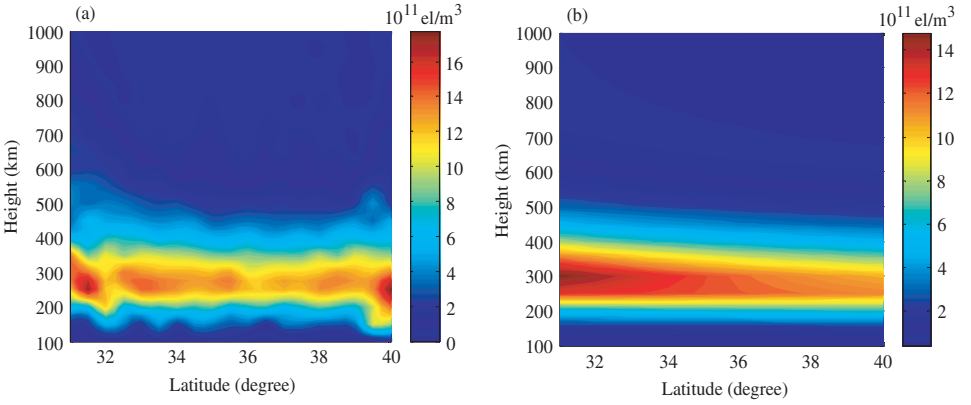

Figure 1. Ionospheric electron density distributions with the latitude of South Korea on 28 October 2003 at UT: 4:00 (LT: 13:00). (a) ground-based GPS tomography reconstruction; (b) IRI-2001.

densities to avoid unreasonable negative values and has been used in this paper. Basically, the MART algorithm is iterated cyclically and can be implemented as the following equation:

$$x_j^{k+1} = x_j^k \cdot \left(\frac{y_i}{a_i . x^k} \right)^{\lambda_k a_{ij}} \tag{6}$$

where y_i is the ith observed STEC in a column of m measurements, x_j is the $_j$th resulted cell electron density in a column of n unknowns, a_{ij} is the length of link i that lies in cell j, λ_k is the relaxation parameter at the kth iteration with $0 < \lambda_k < 1$, and the inner product of the vectors x and a_i is thus the simulated STEC for the ith path. The electron density matrix x is therefore corrected through an iteration by a ratio of the measured STEC and the simulated STEC with a relaxation parameter of λ_k. It is noted that any iterative algorithm requires an initial condition before the iteration begins. Because a limited number of ground receivers over a limited range of zenith angles are available for GPS data collection, such measured STEC data may not be sufficient for the tomography inverse problem. Due to the poor geometry, the initialization could be extremely important for the tomographic reconstruction. In practice, the closer the initial condition is to the true electron density distribution, the more accurate reconstruction will be. Here the IRI-2001 model is used as an initial guess for the tomographic reconstruction.

3. RESULTS AND DISCUSSION. The Korean GPS Network (KGN) with ~80 permanent GPS sites was established in 2000 by Korea Astronomy and Space Science Institute (KASI), Ministry Of Governmental Administration and Home Affairs (MOGAHA), and National Geographic Information Institute (NGII). The continuous GPS observations provide a high resolution STEC of the ray path. The ionosphere is divided into grid pixels at a cell resolution of $0{\cdot}25^\circ \times 0{\cdot}25^\circ$ (in latitude and longitude) and 25 km in height. Electron density profiles can be derived through the tomographic reconstruction techniques, based on the actual data of 30 minutes from all the GPS receivers in the KGN. Figures 1 and 2 show

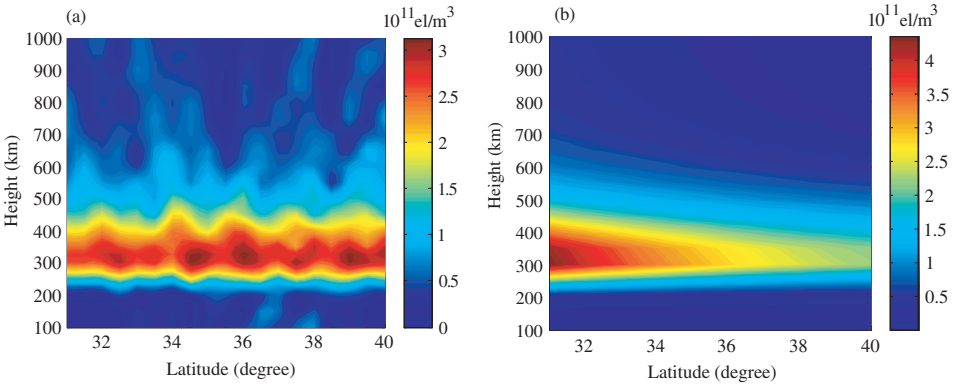

Figure 2. Ionospheric electron density distributions with the latitude of South Korea on 28 October 2003 at UT: 13:00 (LT: 22:00). (a) ground-based GPS tomography reconstruction; (b) IRI-2001.

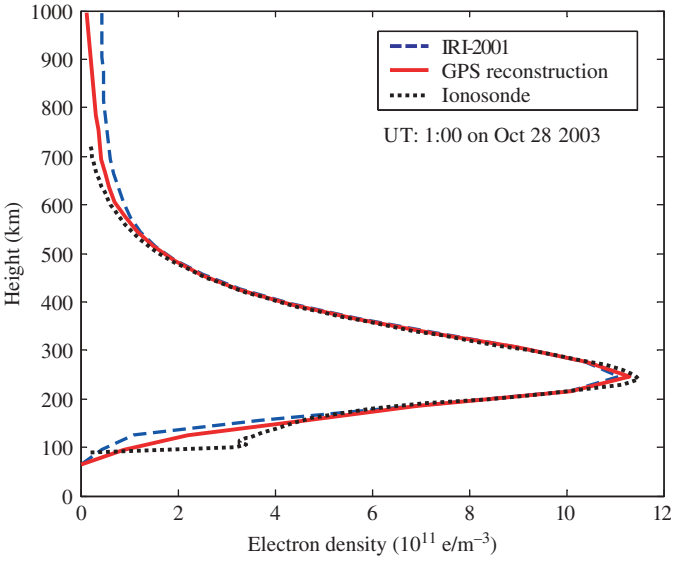

Figure 3. Comparison of the electron density profiles derived from the ground-based GPS tomography reconstruction (solid line), ionosonde observation at Anyang stations (37·39N, 126·95E) (dot line) and IRI-2001 estimation (dash line).

the electron density distributions with height and latitude at longitude 127·0°E in day and night time, respectively, where (a) is the GPS tomography reconstruction and (b) is IRI-2001. It has a consistency between GPS reconstruction and IRI-2001, especially the height of peak electron density. The peak electron density is located in F2 region at about 200–300 km during daylight (see Figure 1) and at about 300–400 km at night (see Figure 2). However there is also an obvious difference between GPS reconstruction and IRI-2001 as the IRI-2001 is an empirical model to give a smooth average ionospheric behaviour.

The available ionosonde station (Anyang) in South Korea provided an independent comparison with the tomographically reconstructed electron density profiles from ground-based GPS observations. Figure 3 is a comparison of the GPS reconstruction results at 01:00 UT (10:00 LT) on 28 October 2003, with the available valid ionosonde data recorded at nearby Anyang station (37·39N, 126·95E) and with density profiles from IRI-2001 model. It shows that the tomographically reconstructed density profile has a good agreement with ionosonde data from Anyang and the IRI-2001 model, but is closer to the ionosonde data, especially in the electron density peak. Although the empirical models, such as IRI-2001, are very useful for giving guidelines for monthly averages of ionospheric behaviour and show diurnal variations well, they cannot reproduce short (minutes to hours) events that occur sporadically. Needless to say these short period events of the ionosphere may affect the normal time density distributions. It is of interest to note that our inversion method can map 3D ionospheric density profile in a short period of time with a good agreement with the independent ionosonde data recorded at the nearby station.

4. CONCLUSION. The empirical IRI models are widely used in many institutes, such as IPS (Ionospheric Prediction Service) radio services in Australia (http://www.ips.gov.au/), as they are very useful for giving smooth-average ionospheric behaviour and show diurnal variations well. However, they cannot be used for short period events related to our daily life. Although the versatility and availability of GPS play an important role in monitoring ionospheric total electron content and space weather, but they are extremely restricted in mapping vertical structure as the ground-based GPS observations are sensitive to the horizontal structure of the ionosphere. Our first result in South Korea, the 3D images of the ionospheric electron density distribution, was derived from the permanent Korean GPS Network (KGN) data. Compared to the profiles obtained by ionosonde data recorded independently at or near the GPS receiver stations, the electron density profiles obtained by the GPS tomographic construction method are in a good agreement with the ionosonde, demonstrating the validity of ionospheric tomography using dense ground-based GPS observations. This good agreement between the independently measured data and our reconstruction density profiles confirms the capability of ionospheric tomography with ground-based GPS measurements.

In the future, it is expected that more data from the dense ground-based GPS receivers and space-based GPS receivers across the concerned region can be used for tomography inversion; and therefore, higher resolution density profiles will be achieved. At that time, the tomography will therefore be a good replacement to ground-based vertically sounding instruments such as radar and ionosonde instruments, as the GPS tomographic reconstruction technique is a comparatively much less expensive technique than radar and ionosonde instruments.

ACKNOWLEDGEMENTS

We are grateful to National Geographic Information Institute (NGII), Ministry of Government Administration and Home Affairs (MOGAHA) and other members who made the observation GPS and ionosonde data available. This work was supported by the Korean Ministry of Science and Technology under grants M2-0306-01-0004, M6-0404-00-0018 and M6-0404-00-0010 and Australian Research Council-linking Project under grants LP0561096.

REFERENCES

Afraimovich, E. Kosogorov, E. A. and Leonovich, L. A. (2000). Determining parameters of large scale traveling ionospheric disturbances of auroral origin using GPS arrays. *Journal of Atmospheric and Solar Terrestrial Physics*, **62**, 553–565.

Afraimovich, E. L Astafieva, E. I. and Voyeikov, S. V. (2004). Isolated ionospheric disturbances as deduced from global GPS network. *Annales Geophysicae*, **22**, 47–62.

Austen, J. R. Franke, S. G. and Liu, C. H. (1988). Ionospheric imaging using computerized tomography, Radio Sci., **23**, 299–307.

Bilitza, D. (2001). International Reference Ionosphere 2000, Radio Sciences, **36**, 261–275.

Ezquer, R. G. Jadur, C. A. and Mostert, M. (1998). IRI-95 TEC predictions for the South American peak of the equatorial anomaly. *Advance in Space Research*. **22**, 811–814.

Gordon, R. Bender, R. and Therman, G. (1970). Algebraic Reconstruction Techniques (ART) for three Dimensional Electron Micoscopy and X-ray Photography. *J.Theor.Biol*, **29**, 471–481.

Jakowski, N. Wehrenpfennig, A. Heise, S. Reigber, C. Lühr, H. Grunwaldt, L. and Meehan, T. (2002). GPS radio occultation measurements of the ionosphere from CHAMP: Early results. *Geophysical Research Letters*, **29**, 951–954.

Jin, S. G. Wang, J. L. Zhang, H. P. and Zhu, W. Y. (2004). Real-time monitoring and prediction of the total ionospheric electron content (TEC) by means of GPS. *Chinese Astronomy and Astrophysics*, **28**, 3, 331–337.

Klobuchar, J. K. (1991). Ionospheric effects on GPS. *GPS World*, 48–51.

Tsai, L. C. Liu, C. H. Tsai, W. H. and Liu, C. T. (2002). Tomographic imaging of the ionosphere using the GPS/MET and NNSS data. *J. Atmos. Sol. Terr. Phys*. **64**, 2003–2011.

Mannucci, A. J. Wilson, B. and Yuan, D N. (1998). A global mapping technique for GPS-derived ionospheric total electron content measurements. *Radio Science*, **33**(3): 565–574.

Otsuka, Y. Ogawa, T. Saito, A. and Tsugawa, T. (2002). A new technique for mapping of total electron content using GPS network in Japan. *Earth Planets Space*, **54**: 63–70.

Reinishch, B. W. Haines, D. M. Benson, R. F. Green, J. L. Sales, G. S; and Taylor, W. (2001). Radio sounding in space: Magnetosphere and topside ionosphere. *J. Atmos. Sol. Terr. Phys*. **63**, 87–98.

Raymund, T. D. Austen, J. R. and Franke, S. J. (1990). Application of computerized tomography to the investigation of ionospheric structures. *Radio Science*, **25**, 771–789.

Ruffini, G. Flores, A. and Rius, A. (1998). GPS Tomography of the Ionospheric Electron Content with a Correlation Functional. *IEEE Transactions on Geoscience and Remote Sensing*, **36**(1): 143–153.

Schaer, S. (1999). Mapping and Predicting the Earth's Ionosphere Using the Global Positioning System. Ph.D dissertation, Astronomical Institute, University of Berne, Switzerland.

Tsunoda, R. T. (1988). High-latitude F-region irregularities: a review and synthesis. *Rev. Geophy*., **26**, 719–760.

Wall, M. E. Dyck, P. A. and Brettin, T. S. (2001). SVDMAN – singular value decomposition analysis of microarray data. *Bioinformatics*, **17**, 566–68.